Investigation of the Summer Climate of the Contiguous United States and Mexico Using the Regional Atmospheric Modeling System (RAMS). Part I: Model Climatology (1950–2002)

CHRISTOPHER L. CASTRO*

Department of Atmospheric Science, Colorado State University, Fort Collins, Colorado

ROGER A. PIELKE SR.

Cooperative Institute for Research in Environmental Sciences, Program in Atmospheric and Oceanic Sciences, University of Colorado, Boulder, Colorado

JIMMY O. ADEGOKE

Laboratory for Climate Analysis and Modeling, Department of Geosciences, University of Missouri—Kansas City, Kansas City, Missouri

(Manuscript received 16 November 2005, in final form 27 November 2006)

ABSTRACT

Fifty-three years of the NCEP–NCAR Reanalysis I are dynamically downscaled using the Regional Atmospheric Modeling System (RAMS) to generate a regional climate model (RCM) climatology of the contiguous United States and Mexico. Data from the RAMS simulations are compared to the recently released North American Regional Reanalysis (NARR), as well as observed precipitation and temperature data. The RAMS simulations show the value added by using a RCM in a process study framework to represent North American summer climate beyond the driving global atmospheric reanalysis. Because of its enhanced representation of the land surface topography, the diurnal cycle of convective rainfall is present. This diurnal cycle largely governs the transitions associated with the evolution of the North American monsoon with regards to rainfall, the surface energy budget, and surface temperature. The lower frequency modes of convective rainfall, though weaker, account for rainfall variability at a remote distance from elevated terrain. As in previous studies with other RCMs, RAMS precipitation is overestimated compared to observations. The Great Plains low-level jet (LLJ) is also well represented in both RAMS and NARR, but the Baja LLJ and associated gulf surges are not.

1. Introduction

Summer climate in North America, and its variability, is strongly influenced by the North American monsoon system (NAMS). The large-scale changes in climate resulting from NAMS development have been thoroughly documented by observational analyses (e.g., Bryson and Lowry 1955; Adams and Comrie 1997; Douglas et al. 1993; Douglas 1995; Higgins et al. 1997a,b; Barlow et al. 1998). Much of this prior work employed global atmospheric reanalyses (GR), such as the National Centers for Environmental Prediction–National Center for Atmospheric Research (NCEP–NCAR) Reanalysis I (Kalnay et al. 1996) or the 40-yr European Centre for Medium-Range Weather Forecasts (ECMWF) Re-Analysis (ERA-40; Uppala et al. 2005). These data are advantageous because they have long records (on the order of 50 years) and are based on atmospheric general circulation models (GCMs) with a fixed dynamical core, physical parameterizations, and data assimilation system. However, because of their coarse resolution and physical parameterizations, the conclusions that can be drawn from such datasets are

* Current affiliation: Department of Atmospheric Sciences, The University of Arizona, Tucson, Arizona.

Corresponding author address: Dr. Christopher L. Castro, Department of Atmospheric Sciences, The University of Arizona, Physics and Atmospheric Sciences Bldg., Rm. 520, 1118 East Fourth Street, Tucson, AZ 85721-0081.
E-mail: castro@atmo.arizona.edu

DOI: 10.1175/JCLI4211.1

limited. This is particularly the case in the warm season because of the dominance of convectively generated precipitation. The recently released North American Regional Reanalysis (NARR; Mesinger et al. 2006) may help to advance our physical understanding of the summer climate. NARR is designed to be a dynamically consistent, high-resolution (32-km grid spacing; 45 vertical levels), high-frequency (3 h) atmosphere and land surface hydrology dataset, though data are available only from 1979 on. More of its particular aspects as relevant to the present study are discussed in section 2. The reanalyses are essentially diagnostic atmospheric models, defined by Pielke (2002) as models that are used in concert with observations via data assimilation. Their primary goal is to obtain the best possible description of the atmosphere and land surface within a consistent framework.

Another tool that has utility in investigation of the summer climate is a regional climate model (RCM). In contrast to a reanalysis, the RCM is used as a process model, in which the goal is to improve understanding of the atmospheric dynamics and thermodynamics. Although comparison of model results to observations is useful in this case, the goal is not necessarily to reproduce the observations. RCMs can be used several frameworks, or dynamical downscaling types, as defined in Castro et al. (2005). In Type 2 dynamical downscaling, for example, an atmospheric reanalysis is used to specify the large-scale forcing to the model. For such simulations, RCMs at present typically use a grid spacing of 10–50 km and a horizontal domain of several thousand kilometers. RCM process studies of North American summer climate thus far fall into one of two types: value-added studies or sensitivity studies.

The value-added studies demonstrate improved representation of mesoscale features in the RCMs, due to better representation of the surface boundary or the dynamics and physics of the model (e.g., Anderson et al. 2000, 2004; Anderson 2002; Berbery 2001; Saleeby and Cotton 2004; Li et al. 2004; Xu et al. 2004). RCMs can improve the representation of the diurnal cycle of convection, the Baja low-level jet (LLJ) and associated gulf surges, the continental out-of-phase relationship in rainfall between the core monsoon region and central United States, and precipitation, though it typically more closely matches satellite observations. Xu et al. (2004), in particular, examined the development of the NAMS onset period during a 22-yr simulation (1980–2001) with the fifth-generation Pennsylvania State University–NCAR Mesoscale Model (MM5) over Mexico and will serve as an important point of reference in evaluating the RCM simulations in this paper.

In sensitivity studies, the surface boundary is changed (soil moisture, vegetation, or sea surface temperature) or the configuration of the RCM (model physical parameterizations, grid spacing, domain size, and/or nudging options) is varied (e.g., Xu and Small 2002; Gochis et al. 2002, 2003; Kanamitsu and Mo 2003; Liang et al. 2004; Miguez-Macho et al. 2005; Castro et al. 2005). There can be large sensitivities to the RCM experimental design, particularly to the choice of convection scheme and nudging options. This can drastically affect the continental-scale distribution of rainfall, for example, such that the monsoon occurs or does not at all (Liang et al. 2004). It is not surprising, therefore, that various RCM solutions for the same time period can be very different, as seen in recent results from the North American Monsoon Model Assessment Project (NAMAP; Gutzler et al. 2004). Such studies provide guidance for constructing an appropriate RCM experimental design for a value-added study and evaluating RCM results.

In terms of this categorization, the present investigation is a RCM process study designed to demonstrate the value added by a particular RCM representation of the summer climate of North America (specifically the contiguous United States and Mexico) for the period 1950–2002. There are three goals that we wish to accomplish: First, demonstrate that the RCM captures essential features of North American summer climate in a Type-2 dynamical downscaling mode. The RCM and NARR will help define what these essential features are, and the NARR provides a consistent target for evaluation of the RCM results. These must then necessarily be present in a seasonal weather prediction mode RCM, or Type-3 dynamical downscaling, in which a GCM is used to supply the lateral boundary forcing to the RCM. This issue is relevant given that recent studies of this type have made specific and dramatic assertions as to how regional climates in North America may change in the future (e.g., Diffenbaugh et al. 2005). Second, present the results for one RCM climatology in a given dynamical downscaling framework, so that it may be compared with other RCMs and suggest a methodology to construct and analyze RCM climatologies for other parts of the world. Third, and perhaps most important, establish the longest RCM summer climatology in North America to date (more than 30 years longer than the NARR) so that long-term climate variability may be evaluated. This topic is treated separately in a companion paper (Castro et al. 2007).

The outline for the paper is as follows. Section 2 gives a description of the RCM and experimental design. Section 3 describes the datasets used for RCM evaluation, including additional detail on the NARR. Section 4 compares the model results against available obser-

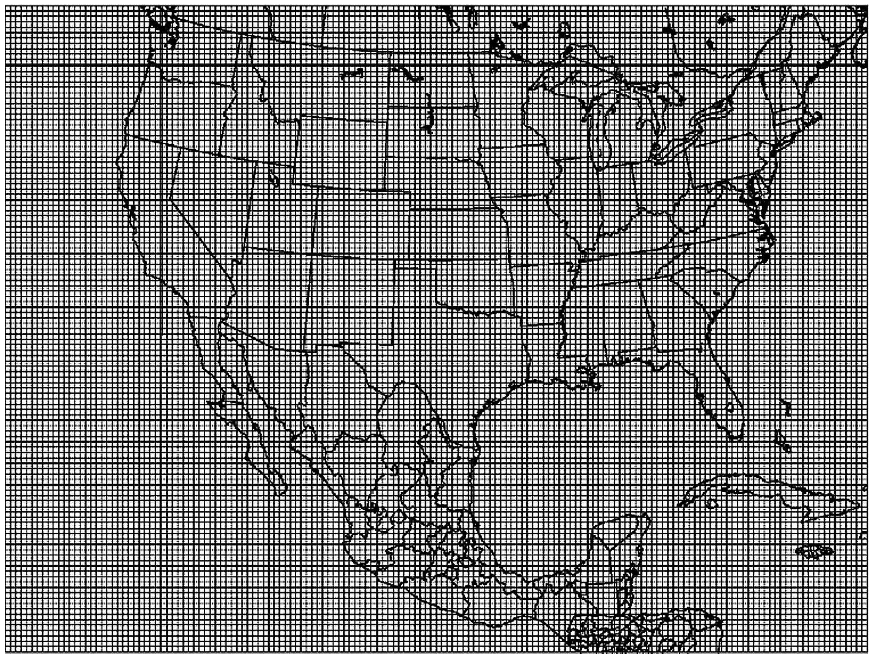

FIG. 1. RAMS domain for North American summer climatology.

vations of precipitation and surface temperature. Section 5 shows additional comparison of model-derived quantities. Section 6 investigates the time-varying modes of atmospheric variability using a spectral analysis technique. A discussion and summary are given in sections 7 and 8, respectively.

2. RCM description and experimental design

a. The model

The model used is the Regional Atmospheric Modeling System (RAMS, version 4.3). This is the same model used by Saleeby and Cotton (2004) in simulating the 1993 North American monsoon season, though the particular model setup here is different. RAMS was originally developed at Colorado State University to facilitate research into predominately mesoscale and cloud-scale phenomena (Cotton et al. 2003; Pielke et al. 1992). It is fully three-dimensional and nonhydrostatic (Tripoli and Cotton 1980). In addition to the study by Saleeby and Cotton, RAMS has demonstrated its utility as a RCM for North America in Eastman et al. (2001), Adegoke et al. (2003), and Liston and Pielke (2001). The model domain (Fig. 1) has horizontal dimensions of 160×120 grid points with a grid spacing of 35 km, encompassing the contiguous United States and Mexico. The model uses a vertically stretched grid with a maximum vertical grid spacing of 1000 m. The minimum vertical grid spacing is 100 m with a vertical stretch ratio of 1.2. There are 30 grid points in the vertical. A modified Kain–Fritsch cumulus parameterization scheme (Castro et al. 2002; Castro 2005), similar to that used in the operational version of the Eta Model, is used to simulate convective precipitation. The Kain–Fritsch parameterization is a mass-flux scheme that accounts for convective updrafts and downdrafts, and cloud liquid and ice phases (Kain and Fritsch 1993; Kain 2004). It has demonstrated a reasonable representation of North American warm season precipitation in other RCMs (Gochis et al. 2002, 2003; Liang et al. 2004) as well as RAMS (Castro et al. 2005). Nonconvective precipitation is simulated by a simple dumpbucket scheme that considers the supersaturation of an air parcel. Other parameterizations are standard for a simulation of this type. Surface fluxes of heat and moisture are represented through the Land Ecosystem Feedback land surface model (LEAF-2) (Walko et al. 2000). Diffusion is parameterized in the horizontal according to Smagorinsky (1963) and in the vertical according to Mellor and Yamada (1974). The radiation scheme is that of Chen and Cotton (1983, 1987).

b. Length of simulations and exterior forcing

The RAMS summer simulations begin 15 May and end 31 August. This interval is sufficient to capture the premonsoon period (15 May to 15 June), the onset of the monsoon (15 June to 15 July), and the peak of the monsoon (15 July to 15 August). Henceforth these definitions will be used to contrast the climate as it evolves during the summer. The NCEP–NCAR GR I is downscaled for 53 years of record (1950–2002). For these simulations, year-specific initial (May) soil moisture and SST data are specified according to the surface datasets described in the proceeding section. The GR geopotential height, temperature, horizontal winds, and relative humidity on standard pressure levels are assimilated at 6-h intervals at regular analysis times. The model uses three-point lateral boundary nudging according to Davies (1976). There is also weak internal nudging at a 1-day time scale, necessary to maintain variability at the large scale when RAMS is run as a RCM (Castro et al. 2005).

c. *Surface boundary specification*

The surface boundary is specified with RAMS products available online from the Atmospheric, Meteorological, and Environmental Technologies (ATMET) Corporation (http://www.atmet.com). This includes U.S. Geological Survey (USGS) topography at 30-min resolution, variable soil type according to the United Nation's Food and Agriculture (FAO) data, and Olson Global Ecosystem (OGE) vegetation datasets. Year-specific sea surface temperatures are from Reynolds and Smith (1994) and are updated monthly. Initial volumetric soil moisture data is prescribed by two datasets. In the part of the RAMS domain that corresponds to the North American Land Data Assimilation System (NLDAS) domain, monthly soil moisture from the Variable Infiltration Capacity (VIC) model is used. VIC is a large-scale hydrologic model run retrospectively over the NLDAS domain for the years 1950–2000 at ⅛° resolution (Maurer et al. 2002). For the years 2001 and 2002, a similar NLDAS product is used. Outside the NLDAS domain, year-specific soil moisture is prescribed by a NCEP global moisture dataset that uses a one-layer hydrologic model described in Huang et al. (1996). At model initialization, soil moisture is assumed constant through the model depth of 2.5 m.

The most optimal way to derive an initial soil moisture condition would be a "spinup" of the model for several months before the period of interest, as in Liston and Pielke (2001). However, this would be very computationally expensive for many years of simulations. To investigate the possible impact of the initial soil moisture assumption, several additional sensitivity experiments were performed for the year 2000: a "cold start" simulation with homogeneous initial soil moisture (at 50% saturation) starting 15 May; a spinup simulation with homogeneous initial soil moisture from 1 January; and a simulation with lateral boundary forcing prescribed by the ECMWF Global Reanalysis with VIC initial soil moisture. In brief, these experiments showed seasonal differences in rainfall that were generally on the order of less than 1 mm day^{-1} between the spinup simulation and that with the initial VIC soil moisture used in the RCM climatology (results not shown). There were much larger differences in rainfall for the cold start simulation and simulation using the ECMWF GR. Therefore, given the objectives of the present study and the uncertainties in the lateral boundary forcing, the initial soil moisture assumption is probably good enough. It is also likely better than using the corresponding GR soil moisture as an initial condition (e.g., Xu et al. 2004).

3. Datasets for RCM evaluation

a. *Observations*

The observed daily precipitation gauge data are from the U.S. Climate Prediction Center (CPC) real-time and retrospective dataset (Higgins et al. 1996). These data span the period 1950–present and encompass all of the contiguous United States and Mexico. Daily satellite-derived precipitation is considered from three sources available from the NASA Goddard Distributed Active Archive Center: 1) the Global Precipitation Climatology Product (GPCP), which is a combined satellite and gauge product; 2) the Arkin and Janowiak Goddard Earth Observing Satellite (GEOS) precipitation index (GPI; Arkin 1979); and 3) the Tropical Rainfall Measuring Mission (TRMM). All of these datasets were used for the period 1998–2004 when daily data are available. Observed surface temperatures over land are taken from global summary of the day (SOD) data over the United States and Mexico.

b. *NARR*

The description of the NARR, as relevant to the present study, is briefly expanded here. NARR is based on the NCEP version of the Eta Model and data assimilation system, which includes the NOAH land surface model. Its lateral boundary conditions are supplied by the NCEP–Department of Energy (DOE) GR (NCEP Reanalysis II; Kanamitsu et al. 2002). Additional data assimilated into the NARR include CPC and GPCP observed precipitation, near-surface winds and moisture, and satellite-derived temperatures. See Mesinger et al. (2006) for further details. All RAMS RCM results are presented alongside the NARR equivalents. Henceforth both are referred to as "models" when referencing their results. It should be expected a priori that NARR would yield the "better" results if the goal is strictly comparison with observations since it is a diagnostic model.

4. Comparison of model results to observations

a. Precipitation

There are several a priori expectations as to where the enhanced surface boundary of a RCM should add value to the climatology of precipitation and atmospheric moisture beyond an atmospheric reanalysis. First, it should be expected that the RCM should yield a better representation of rainfall as the summer season progresses. Analysis of radar data shows that rainfall becomes less dependent on large-scale synoptic weather systems and more dependent on diurnally forced convection or propagating mesoscale convective systems as the summer proceeds (Carbone et al. 2002). Second, rainfall should be more realistically represented in locations where the diurnal cycle of convection is dominant, arising from complex topography and/or land–sea contrast. These are also areas where periodic surges of moisture occur due to LLJs. Finally, it should be expected that precipitation should improve in areas where land surface feedback may be important. For these reasons, the focus here will be on the core monsoon region [defined as the U.S. Southwest (SW) and northwest Mexico] and the central United States.

The observed gauge- and satellite-derived precipitation products are shown in Fig. 2. The features in the CPC gauge-derived precipitation are well known and have been previously described (e.g., Higgins et al. 1999). In the premonsoon period, there is a maximum of precipitation in the central United States. The principal moisture source for this precipitation is the Great Plains (GP) LLJ, which is strongest at this time relative to the latter part of the summer. In Mexico, the NAMS advances northwestward along the Sierra Madre Occidental (SMO) into the core monsoon region as the summer proceeds. In the southwest United States, during the premonsoon period there is little, if any rainfall, and hot, dry conditions. By July, the typical monsoon pattern develops across the continent. According to Higgins et al. (1999), monsoon onset in the core monsoon region occurs sometime between late June and early July with a sudden increase in rainfall, on the order of 50 mm per month in the southwest United States and more than 100 mm per month along the SMO. The maximum rainfall amounts occur on the crests of the mountain ranges, like the SMO and the Mogollon Rim in Arizona. Correspondingly, during the peak of the monsoon, there is a decrease in rainfall in the central United States, particularly in the southern Great Plains where rainfall decreases 50 to 75 mm per month. In the southeast United States, there is a slight increase in rainfall following the monsoon onset in the southwest United States. This monsoon pattern of precipitation is maintained through August. GPCP yields nearly identical results. It is important to note, however, that other gauge-based precipitation data suggest that the CPC and GPCP products may be underestimating the summer rainfall in western Mexico, especially in the SMO (T. Cavazos 2005, personal communication).

The purely satellite-derived precipitation products (results shown south of 40°N in Fig. 2) are more varied in their precipitation estimates. The TRMM data correspond fairly well with CPC and GPCP. However, the GPI product provides a higher estimate, particularly in western Mexico where the difference is in the range of 100 mm per month. Similar discrepancies in satellite versus gauge data were reported by Li et al. (2004). Differences may be accounted for by the specific algorithms to derive rain rate. The GPI algorithm tends to perform poorly in areas with a high coverage of cirrus clouds. This may explain why the rainfall maximum in western Mexico is shifted a bit farther west than observations. In spite of these differences in rainfall amounts, both GPI and TRMM capture the evolution of summer rainfall from the premonsoon to monsoon peak period well.

Modeled precipitation is shown in Fig. 3. NARR precipitation, not surprisingly, is virtually identical to CPC and GPCP since these data are being assimilated. RAMS precipitation shows a similar pattern, though there are important differences. As in observations, RAMS captures the premonsoon maximum in precipitation in the central United States and the onset of the North American monsoon in the core monsoon region. In western North America, the precipitation is clearly tied to the topography, with a greater amount of precipitation occurring with higher elevation. In general, the model in its configuration tends to overestimate total precipitation throughout the entire domain when compared to gauge data. It overestimates most in the southeast United States and Mexico, with rainfall errors approaching 100 mm in a month, on the same order as the difference in the GPI product with CPC. An exception to this is the western part of the NAMS region (western Sonora and western Arizona), where precipitation is slightly underestimated. This may be a result of the model underestimating the strength of moisture flux from the Gulf of California into this region, to be discussed in section 4.

The corresponding NCEP and ECMWF GR precipitation is also shown in Fig. 3. In contrast to the RAMS and observed precipitation, neither captures the seasonal evolution of precipitation well. The NAMS does not properly advance northwestward along the SMO and into the core monsoon region. The core of maxi-

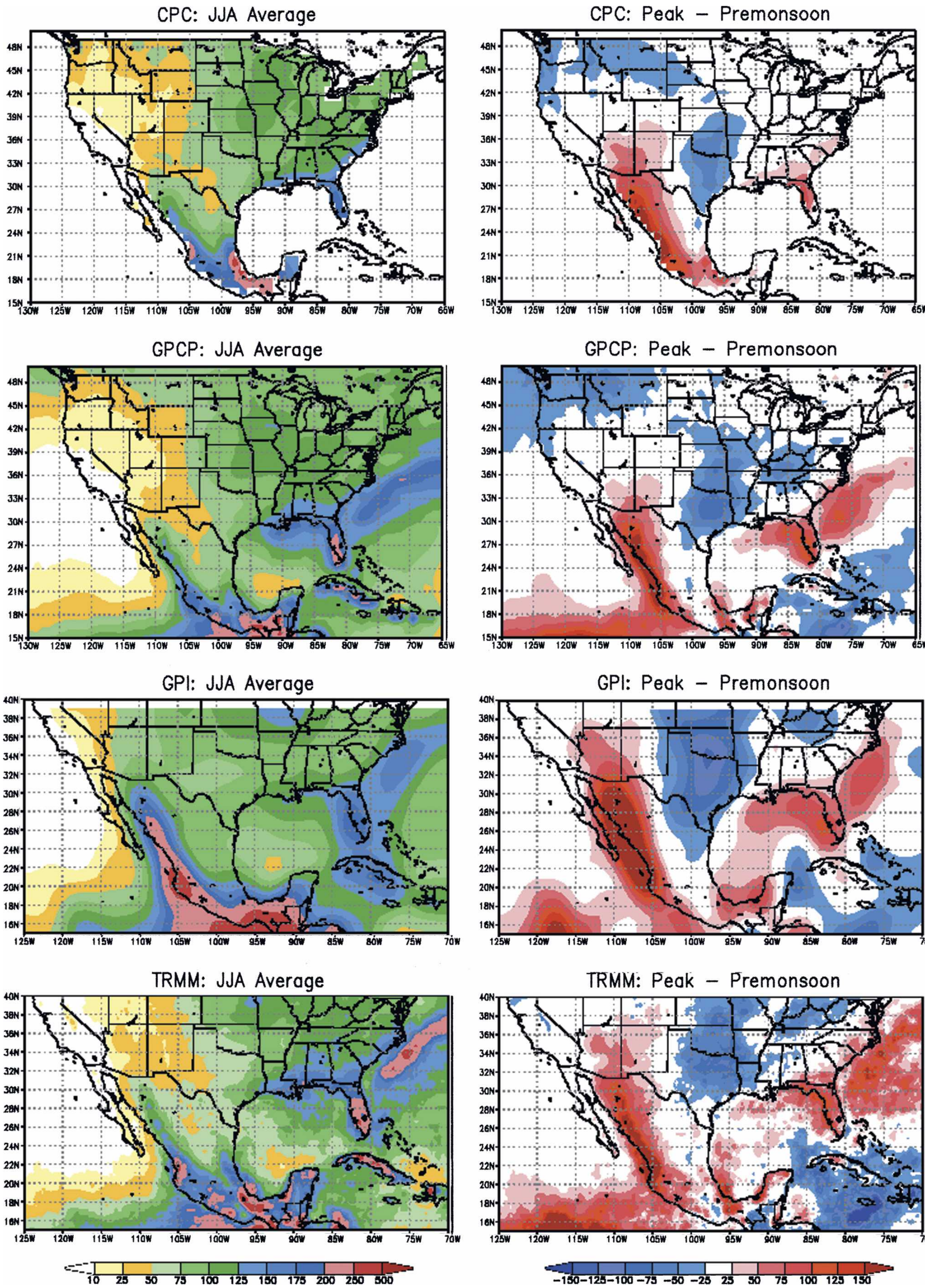

FIG. 2. Observed average precipitation (mm) for the summer months and the difference between the monsoon peak and premonsoon periods for gauge- and satellite-derived datasets. Shading indicated by color bars.

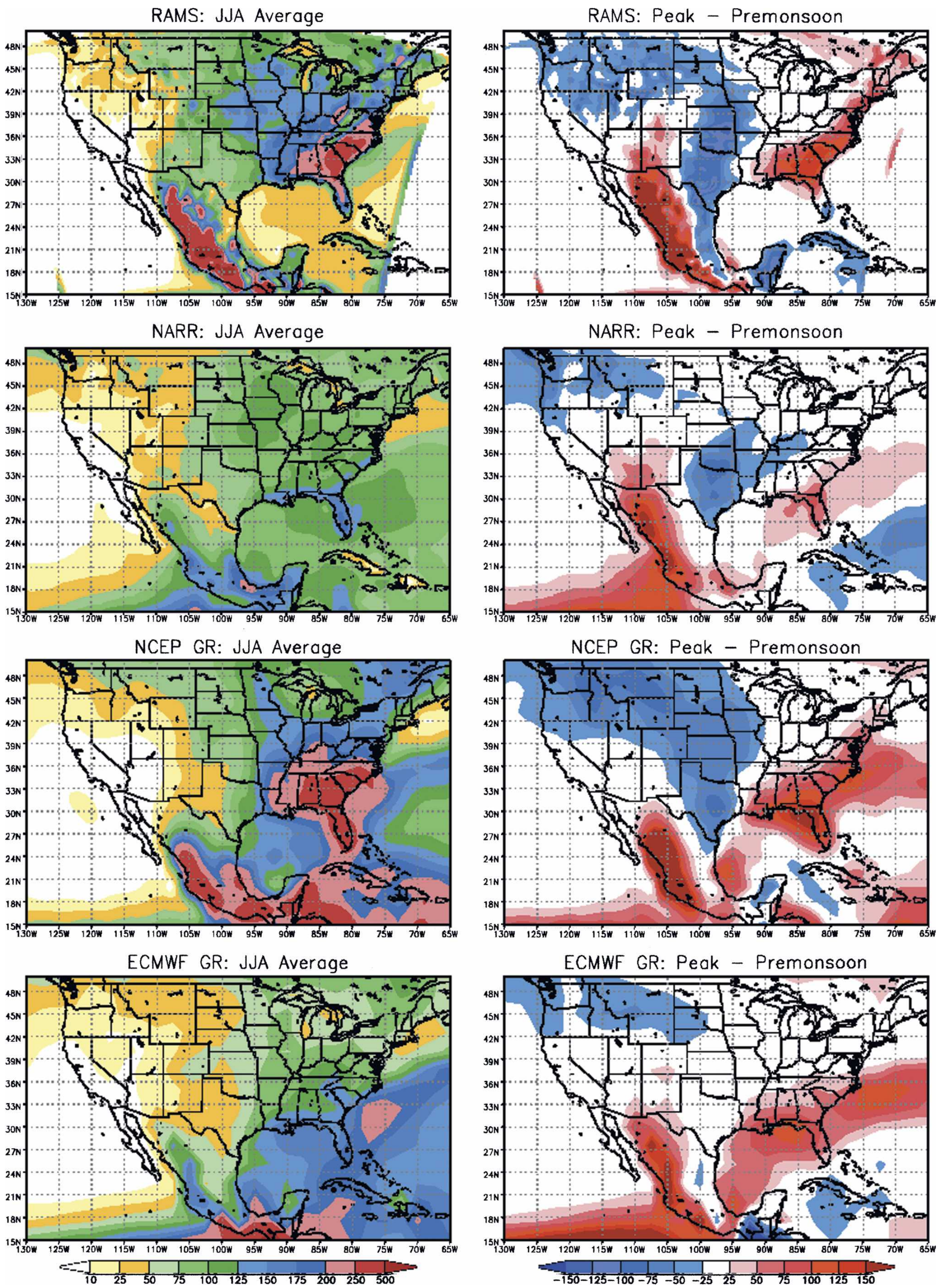

FIG. 3. As in Fig. 2 but for RAMS, NARR, NCEP GR, and ECMWF GR.

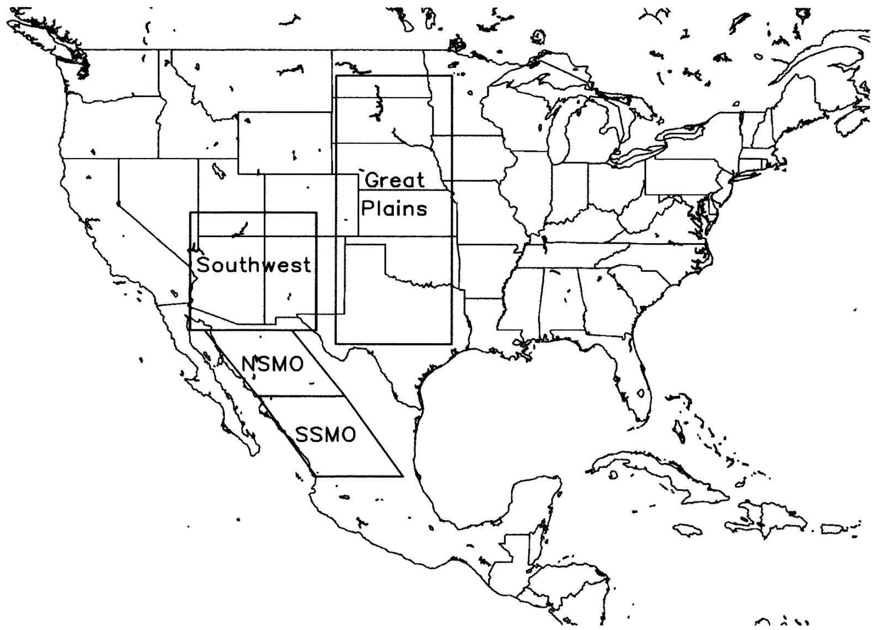

Fig. 4. Selected regions used in considering the time evolution of temperature and precipitation.

mum rainfall (greater than 100 mm per month) fails to reach the state of Sonora in northwest Mexico. In the eastern United States, beyond the Great Plains, rainfall in the NCEP GR is overestimated through the entire summer as compared to gauge data. An overestimation of atmospheric moisture as provided by the NCEP GR to RAMS may be the cause of the excessive RAMS precipitation in this area. In the Great Plains itself, however, precipitation is underestimated, particularly in the latter part of the summer. The ECMWF GR does not capture the decrease in precipitation as the summer proceeds. Overall, the GRs represent precipitation worst in areas where the NAMS has the greatest influence on precipitation. Not surprisingly, similar results exist in GCM simulations (e.g., Yang et al. 2003).

To further investigate the timing and amount of precipitation in the core monsoon region and central United States, the time evolution of daily average precipitation for the GP, SW, northern Sierra Madre Occidental (NSMO), and southern Sierra Madre Occidental (SSMO) is considered. The locations of these regions are shown in Fig. 4. The GP and SW regions are nearly identical to those in Castro et al. (2001). The observational products are first considered in Fig. 5a. These show a dry premonsoon period in the core monsoon region with a sudden jump in precipitation during the onset period. The onset period agrees with Higgins et al. (1999). The differences between GPI and the other products become most apparent during this time. In the NSMO, in particular, the precipitation amount estimated by GPI is about double that of CPC (6 versus 3 mm day^{-1}). Meanwhile, precipitation in the GP gradually decreases following onset (by about 1 to 2 mm day^{-1}).

The corresponding regional model and GR precipitation are shown in Fig. 5b. The GR precipitation worsens as the summer proceeds. In particular, Fig. 5b clearly shows that the sudden increase in precipitation during the monsoon onset period does not occur in the NSMO and SW. Precipitation in the SW remains virtually unchanged through the entire summer and there is no monsoon at all. As mentioned, the ECMWF GR also shows no decrease in GP precipitation through the summer. RAMS increases the precipitation in all regions and shows that a RCM can improve upon the reanalysis in some regions. Most important, RAMS captures the sudden jump in precipitation in the NSMO and SW regions at monsoon onset. The evolution of precipitation in the GP, NSMO, and SW is close to that depicted by the GPI product and within 1 mm day^{-1} of the NARR in the GP and SW. The one region in which RAMS appears to degrade the precipitation estimate is the SSMO, where the NCEP GR already overestimates precipitation. RAMS precipitation in Mexico is similar to estimates with different RCMs (e.g., Xu et al. 2004). The comparison of precipitation between observational and model products demonstrates that the higher resolution of the RCM is necessary to capture the abrupt

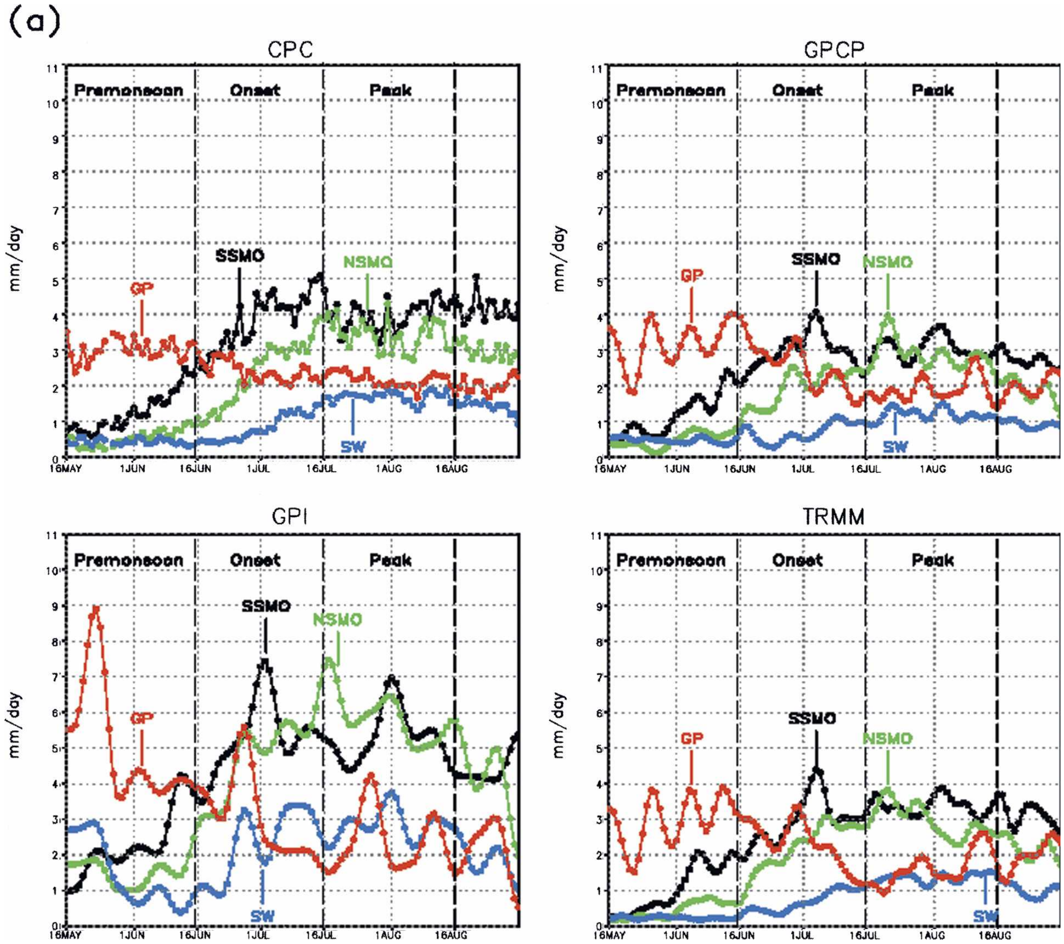

FIG. 5. Evolution of average observed precipitation (mm day^{-1}) for regions identified in Fig. 4 for (a) observed datasets and (b) RAMS, NARR, NCEP GR, and ECMWF GR: Premonsoon, monsoon onset, and monsoon peak periods identified.

transitions in North American climate associated with development of the monsoon.

b. Surface temperature

June–August averaged surface temperature from RAMS and NARR along with the difference between monsoon peak and onset periods is shown in Fig. 6. The most striking feature in RAMS temperatures is the maximum in the Colorado River valley matching the climatological position of the surface heat low that forms in this location. The local maximum in average surface temperature is greater than 306 K. The NARR surface temperatures are warmer throughout the Great Plains and U.S. Southwest by 2–4 K. In spite of this difference in mean temperature, both models show that surface temperature decreases in northwest Mexico by 1–3 K after monsoon onset. While this occurs, temperatures in the surrounding areas increase.

The time evolution of average surface temperature, including SOD data, through the summer season for the regions in Fig. 4 is shown in Fig. 7. In all monsoon regions, the SOD data indicate that surface temperatures increase until monsoon onset, then gradually decrease. The observed temperature decreases are more dramatic in Mexico, especially in the NSMO (3–4 K) due to the abrupt shift in rainfall. The average surface temperature in the Great Plains tends to increase to a maximum of 300 K in mid-July, then decrease into August. As compared to the SOD data, there is a cold bias in RAMS for all of the regions, which may reflect the fact that RAMS is overestimating the precipitation. RAMS and NARR show a decrease in surface temperature in the SMO following monsoon onset, but not in the U.S. Southwest, in contrast to Xu et al. (2004). The NARR, quite surprisingly, has a warm bias in surface temperature in the Southwest and Great Plains

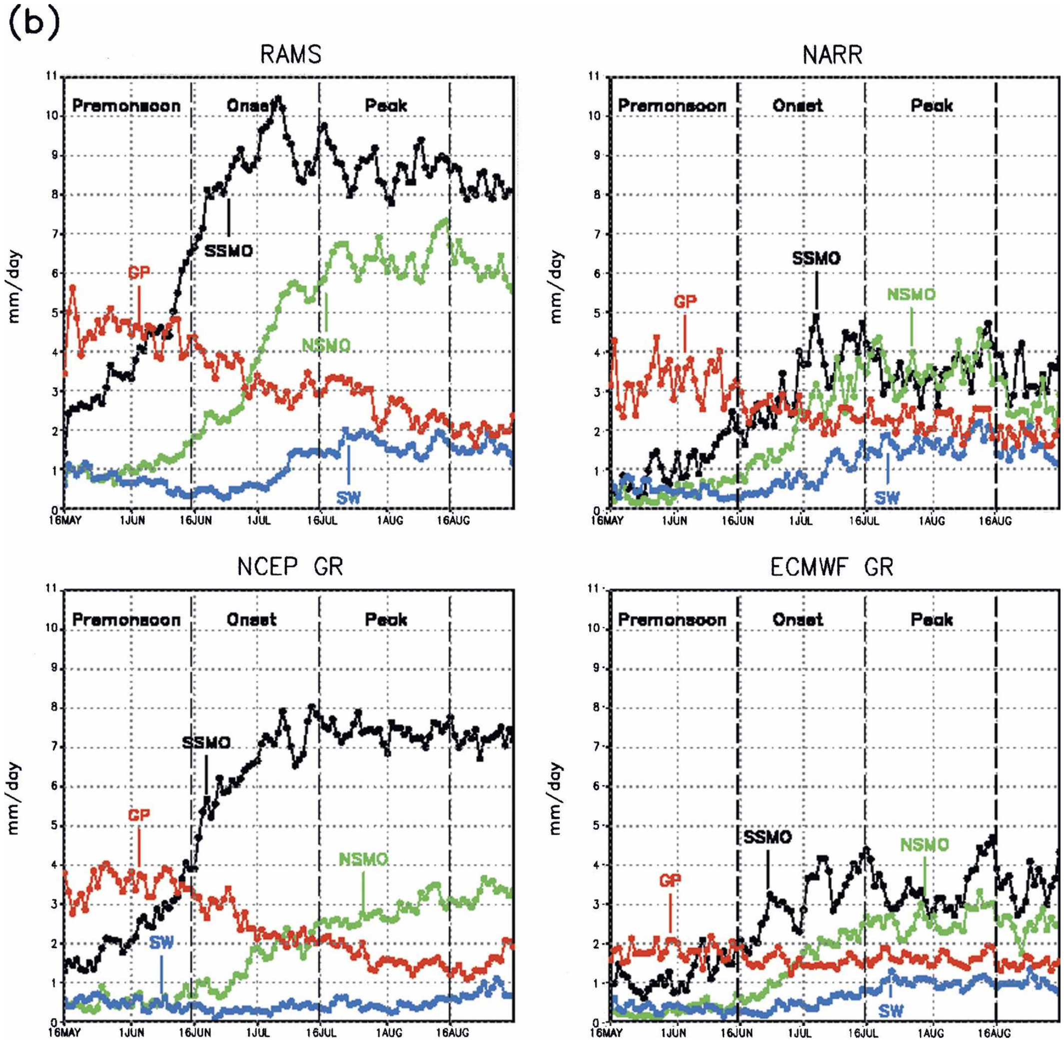

FIG. 5. (*Continued*)

(2–4 K), especially during the latter part of the summer. RAMS provides better representation of surface temperature for those regions.

5. Comparison of model-derived quantities

a. Surface moisture flux

Figure 8 shows the surface moisture flux. The surface moisture flux is considered instead of the total integrated moisture flux to better highlight the Great Plains and Baja LLJ. It has been noted that the Great Plains LLJ is well represented by the NARR, and our own analysis with SOD-derived surface moisture flux (Castro 2005) obtained nearly identical results for its magnitude (on the order of g kg^{-1} 60–80 m s^{-1}). RAMS overestimates the strength of the Great Plains LLJ by about 10%–20%, but its seasonal evolution is well represented. As the summer proceeds, the Baja LLJ increases in strength, and much of its variability occurs due to periodic gulf surge events, such as demonstrated by Berbery (2001) and Berbery and Fox-Rabinovitz (2003). Surges are characterized by southeasterly winds through the Gulf of California, so that the total wind vector is parallel to the coast. The Baja LLJ in the NARR is dramatically overestimated, and this serious problem has been previously documented (Mo et al. 2005). The climatological magnitude (100 g kg^{-1} m s^{-1}) and orientation of the surface moisture flux reflecting the Baja LLJ in the NARR is about the same as observed during a strong gulf surge event in the North American Monsoon Experiment (NAME; Rogers 2005). By contrast, the magnitude of the RAMS average surface moisture flux is much closer to that observed (40–60 g kg^{-1} m s^{-1}). However, RAMS tended

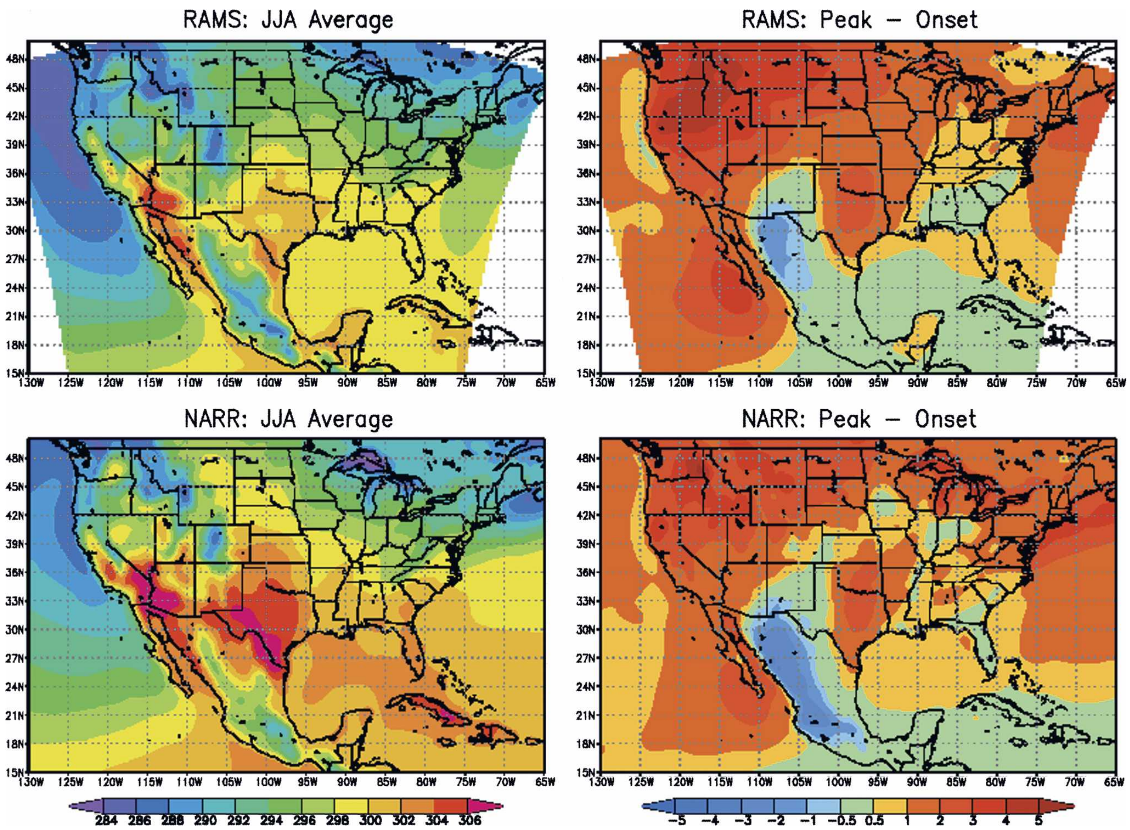

FIG. 6. Average surface temperature (K) for the summer months and the difference between the monsoon peak and monsoon onset periods for RAMS and NARR. Shading indicated by the color bars.

to underestimate the strength of gulf surges and never produced southeasterly winds in the Gulf of California. We examine this issue further in section 6 and suggest reasons for the incorrect representation of the Baja LLJ in RAMS.

b. The 700-mb wind

The monthly average 700-mb winds (Fig. 9) are nearly identical to the Xu et al. (2004) climatology and NCEP GR. These results are not very surprising given that RAMS is being nudged in its interior. Though not shown, a similar result exists for the evolution of 500-mb height (e.g., Castro et al. 2001). The 700-mb winds reflect the northwestward advancing anticyclonic circulation that centers itself over the U.S. Southwest during July and August. To the south of this anticyclonic center, winds are easterly. At this time, the zero mean zonal wind line reaches into Arizona and New Mexico, but easterlies can periodically penetrate farther northward with the passage of disturbances around the southern periphery of the ridge. In the monsoon regions identified earlier, the switch to easterly flow at 700-mb generally corresponds to monsoon onset. This suggests that most of the upper-level moisture for the monsoon is originating from the Gulf of Mexico after onset, in agreement with previous GR studies (e.g., Schmitz and Mullen 1996). It is also opposite to the direction of the surface moisture flux in Fig. 8, which suggests a low-level monsoon moisture source (below 700 mb) of the Gulf of California or east Pacific.

c. Sensible and latent heat fluxes

The average summer sensible and latent heat fluxes and the difference between the monsoon peak minus premonsoon period are shown in Fig. 10. For both RAMS and NARR, the surface heat fluxes reflect the evolution of surface temperatures shown in section 3b, and the largest changes are found in the south-central United States and core monsoon region. During the premonsoon period there is a maximum in sensible heat flux in the Sonoran desert (RAMS has an additional maximum on the east coast of Mexico). In the south-central United States, most of the surface energy is being partitioned into latent heat (about 200 W m^{-2} in RAMS), which confirms that this region is an important moisture source for precipitation (Brubaker et al.

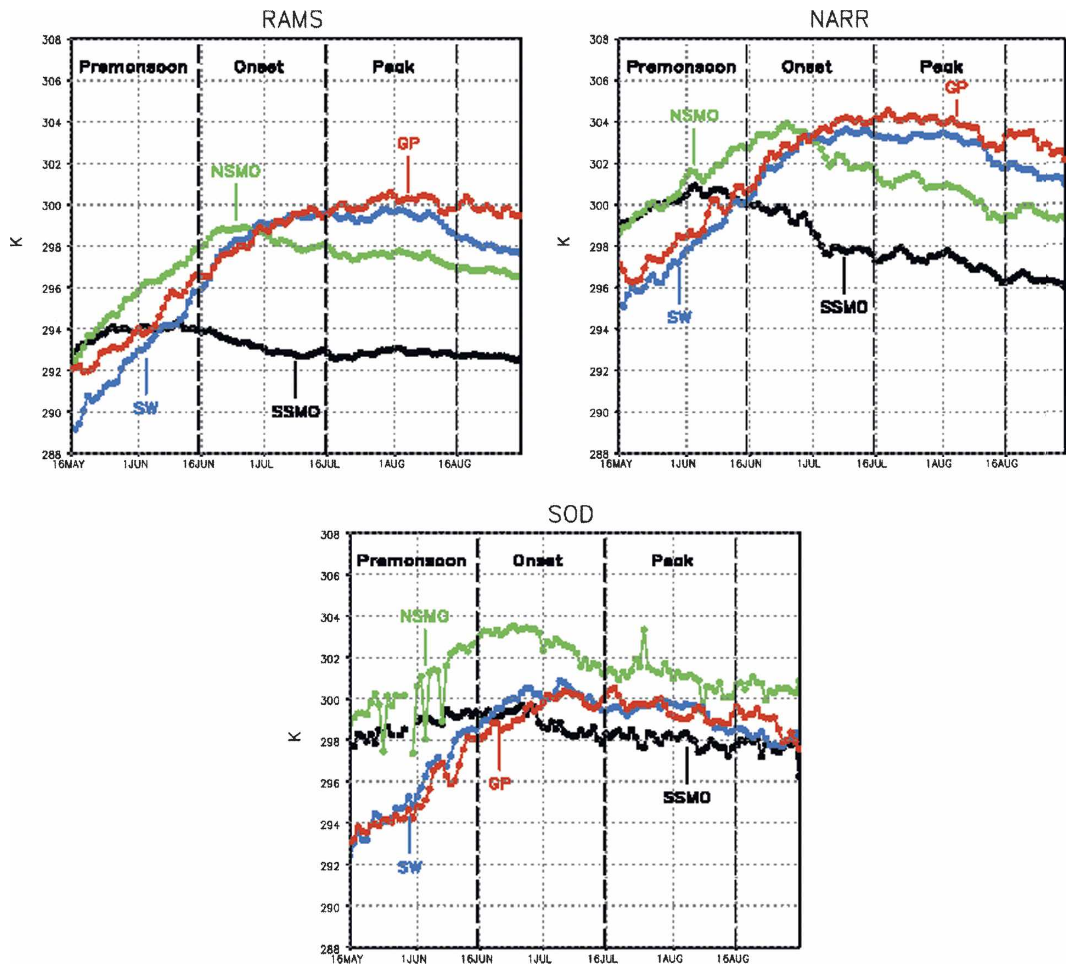

FIG. 7. As in Fig. 5 but for average surface temperature (K) for RAMS, NARR, and SOD.

2001). The magnitude of the latent heat flux in this region is less in the NARR (by about 40 W m^{-2}) because less rainfall occurs compared to the RAMS simulations. After monsoon onset, the latent heat flux decreases and the sensible heat flux increases as the soil moisture dries out. The core monsoon region can be divided into two parts with distinct behavior with respect to surface heat fluxes. In areas with the heaviest rainfall, like the SMO in Mexico, the sensible heat flux decreases after monsoon onset. To the north and west, in the southwest United States and northwestern Sonora, even though rainfall increases after monsoon onset, it is less, and more, intraseasonally variable (see section 6). So the sensible (latent) heat fluxes do not change their tendency to increase (decrease) as the summer proceeds. This would explain why modeled surface temperatures do not decrease following monsoon onset in the southwest United States (Fig. 7). It is also worth noting that the largest values of latent heat flux in the NARR (more than 200 W m^{-2}) occur in the Gulf of California.

6. Spectral analysis of integrated moisture flux convergence

As a proxy for convection in the model, we use model-integrated moisture flux convergence (MFC) (e.g., Castro et al. 2005):

$$\mathrm{MFC} = -\frac{1}{g}\int_{p_{\mathrm{top}}}^{p_s} \nabla(q\mathbf{v})\,dp, \qquad (1)$$

where q is the specific humidity, $\mathbf{v}$ is the horizontal wind vector, and p is the pressure; p_s and p_{top} correspond to the surface pressure and pressure at the model top (or 100 mb in the NARR), respectively. MFC is used, in lieu of precipitation, because it is more closely related to the model dynamics and less influenced by the convective parameterization. It is also available from

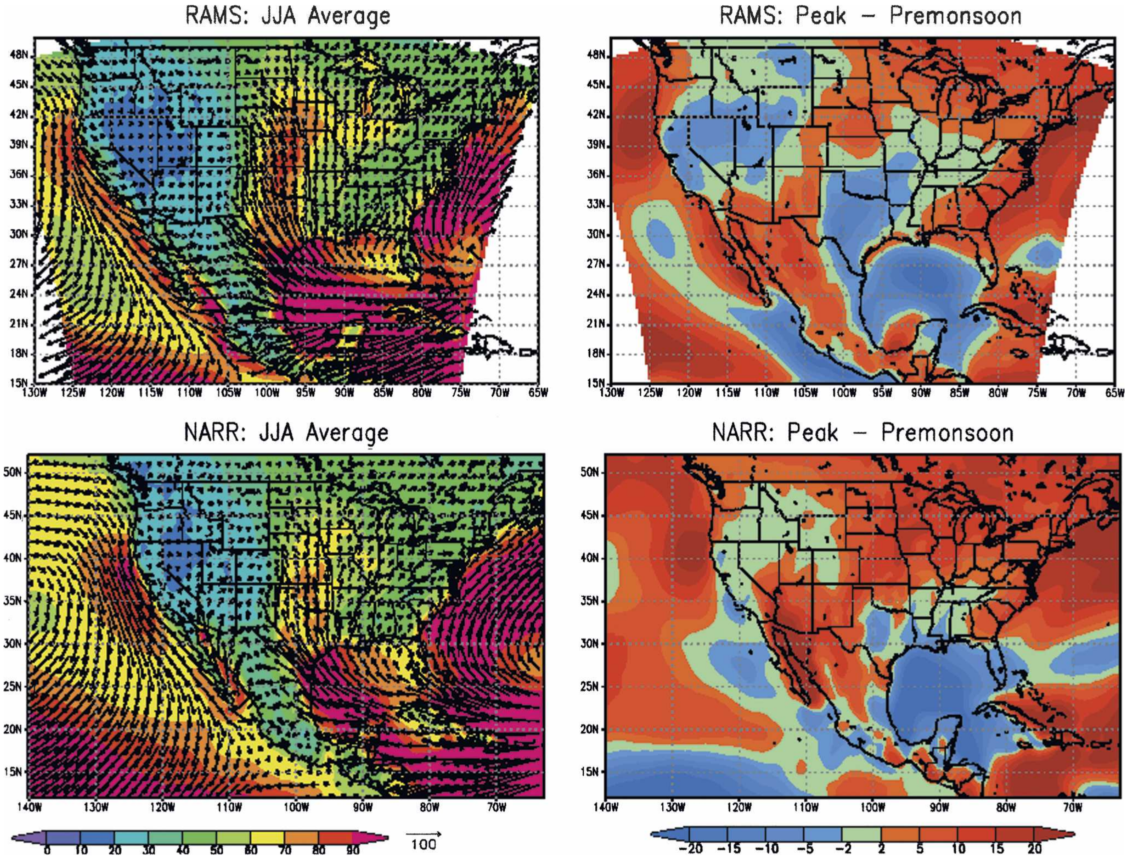

FIG. 8. Average surface moisture flux (g kg^{-1} m s^{-1}) for the summer months and the difference between the monsoon peak and monsoon onset periods for RAMS and NARR. Vector length is 100 g kg^{-1} m s^{-1}. Shading indicated by color bars.

RAMS and NARR at a time interval necessary to capture the diurnal cycle (6 and 3 h, respectively, for each). The spectral power of MFC per wavenumber k for a given 30-day period (S_k) is computed using a conventional Fourier analysis technique (e.g., von Storch and Zwiers 1999). The formulation of Gilman et al. (1963) is used to compute the red noise spectrum (ϕ_k). A complete description of the mathematical details is given in Castro (2005). Similar spectral decomposition approaches have been done using RCM data (Berbery and Fox-Rabinovitz 2003) and radar observations (Carbone et al. 2002).

The spectral power (S) in a given band k_1 to k_2 is

$$S = \sum_{k_1}^{k_2} (S_k)\left(\frac{2\pi}{N}\right). \tag{2}$$

This is multiplied by a weighting factor (W) that accounts for the area that is above a red noise spectrum. The weighting factor is determined in the following way. First, the integrated spectral power in the band exceeding red noise (A_+) is calculated. If $S_k > \phi_k$ for k in the band k_1 to k_2, then

$$\sum_{k_1}^{k_2} (S_k - \phi_k)\left(\frac{2\pi}{N}\right) = A_+. \tag{3}$$

Next, the total area above and below the red noise spectrum (A_{tot}) is

$$\sum_{k_1}^{k_2} |S_k - \phi_k| \frac{2\pi}{N} = A_{tot}. \tag{4}$$

The weighting factor is then $W = A_+/A_{tot}$: $W = 1$ means that all the spectral power in the band exceeds red noise and $W = 0$ means that all the spectral power in the band is below red noise.

For a given 30-day period, the average integrated climatological spectra (S) is weighted by the fraction of spectral power above the climatological red noise spectrum in a given frequency band (W). The weighting ensures that the most physically relevant features are emphasized. We henceforth refer to the quantity WS as

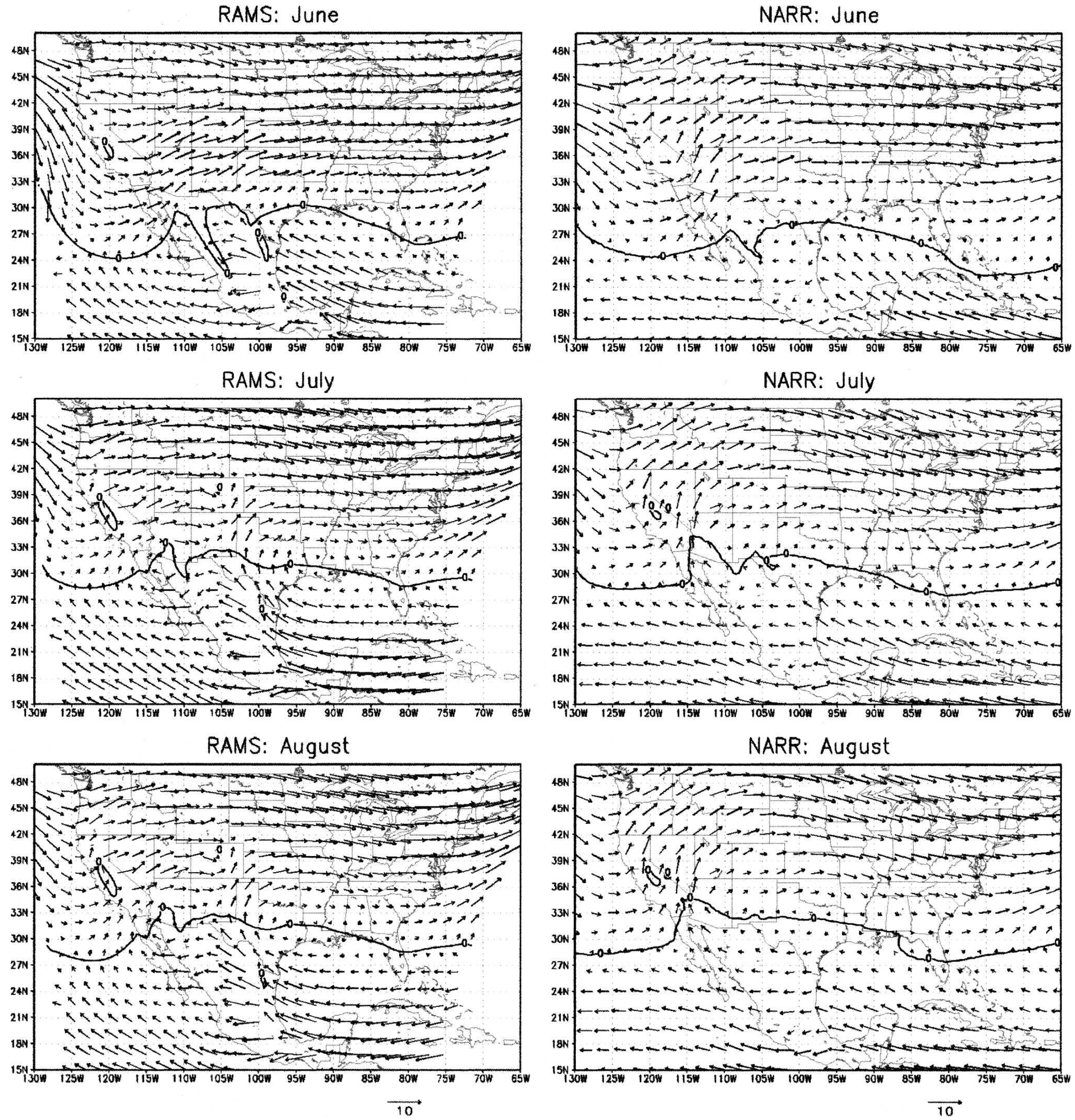

FIG. 9. Average 700-mb wind vectors for the summer months for RAMS and NARR. The average zero mean zonal wind line is indicated by a solid line. Vector length is 10 m s^{-1}.

the weighted spectral power. Three distinct frequency bands are specified by the distinct behavior of MFC: a synoptic mode (4–15 days), a subsynoptic mode (1.5–3 days), and a diurnal mode (1 day).

Figure 11 shows the averaged weighted spectral power of MFC in the diurnal band for the summer months and the monsoon minus premonsoon period. With a few exceptions, the magnitude and spatial pattern of the diurnal cycle is fairly consistent between RAMS and NARR. The weighted spectral power is positive throughout the entire domain and largest where there are terrain gradients and areas of land–sea contrast. The strongest diurnal signal (greater than 50 mm^2 day^{-2}), not surprisingly, occurs in central and southern Mexico. This maximum advances northwestward along the SMO with the monsoon. Another maximum in the diurnal cycle occurs on the eastern side of the Rocky Mountains in Colorado and extends into the Great Plains, reflecting the nocturnal peak in convection there. In the southeast United States, there is a diurnal cycle tied to a sea breeze circulation, particularly in Florida. RAMS appears to overestimate the strength of the diurnal cycle in the Appalachians, and this leads to the large overestimate in rainfall there. The

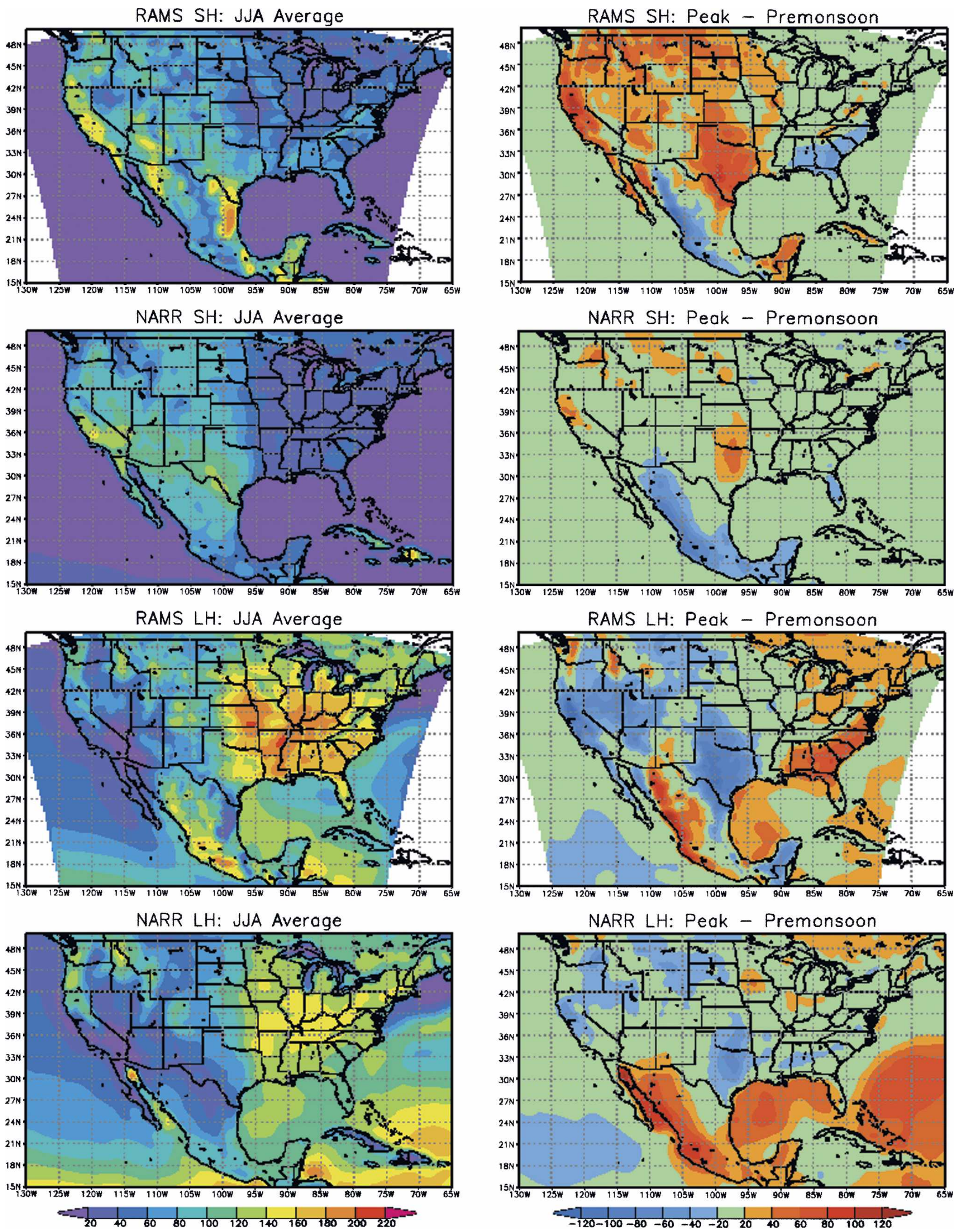

FIG. 10. Average monthly sensible and latent heat fluxes (W m^{-2}) for the summer months and the difference between the monsoon peak and premonsoon periods for RAMS and NARR. Shading indicated by the color bars.

difference in diurnal MFC between the monsoon and premonsoon periods mirrors the large-scale changes in rainfall shown in section 2. There is an increase in the strength of the diurnal cycle in western Mexico and the southwest United States, and a decrease over the southern Great Plains and northeast Mexico. Though the diurnal convection is locally forced, its strength is modulated by the large-scale circulation. The magni-

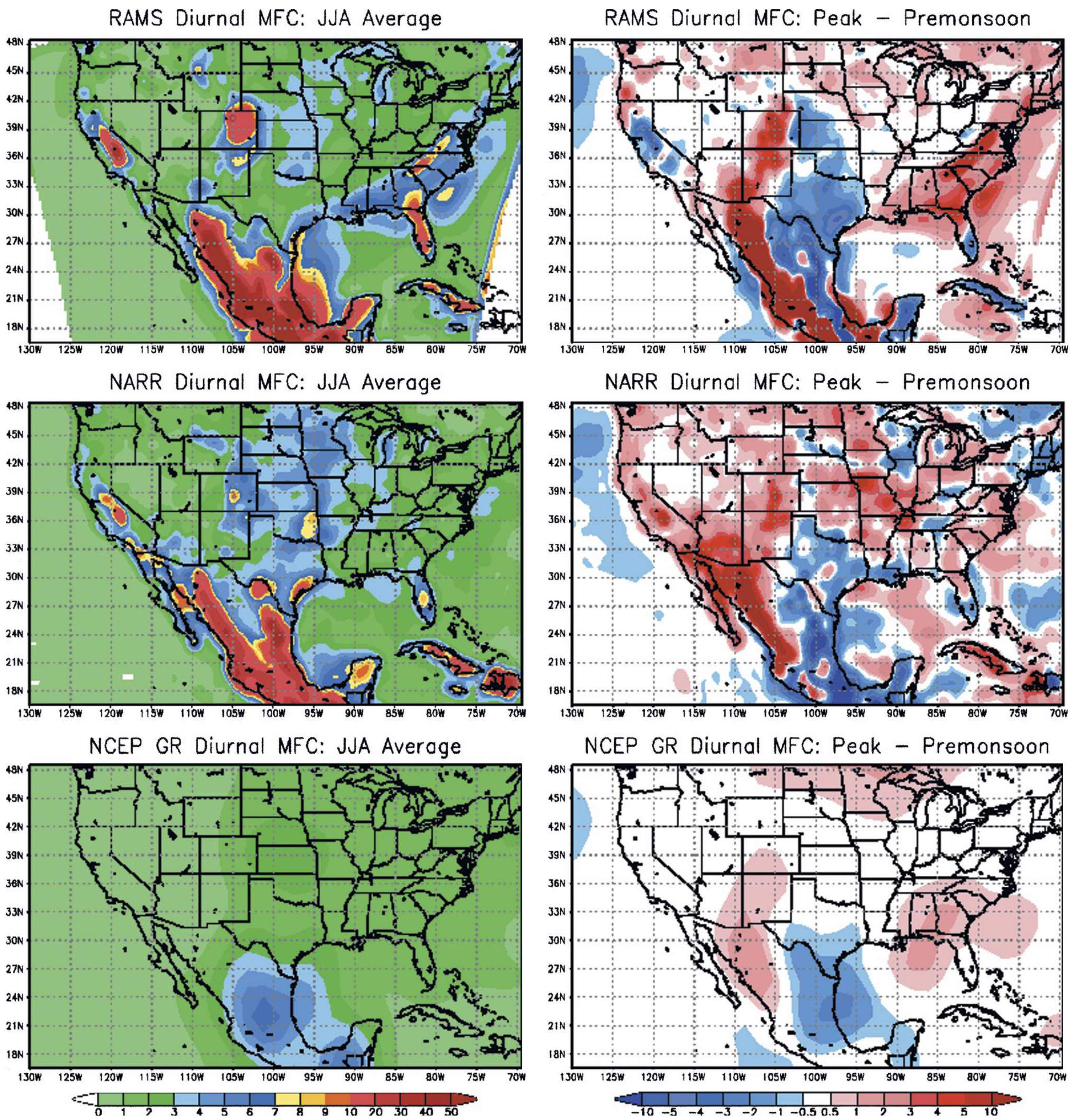

FIG. 11. Weighted spectral power of MFC ($mm^2\ day^{-2}$) in the diurnal band for the summer months and the difference between the monsoon peak and premonsoon periods for RAMS, NARR, and NCEP GR. Shading indicated by the color bars.

tude of the diurnal cycle of MFC is about 10 times weaker in the NCEP GR (bottom of Fig. 11). The GR rainfall is most profoundly impacted in areas where the diurnal cycle is the dominant mechanism for summer rainfall, in this case the core monsoon region and the central United States. Therefore, increased resolution of the complex terrain in western North America is crucial for a reasonable representation of the NAMS.

The other modes of variability in MFC are much weaker in strength than the diurnal cycle but are still physically important and display distinct spatial patterns. The subsynoptic component (Fig. 12), unlike the diurnal cycle, has virtually no weighted spectral power in the western United States, southeast United States, or Mexico. Virtually all of the variability in this band occurs east of the Rocky Mountains. In RAMS it can be approximately equal to or slightly more than the magnitude of the diurnal cycle but is weaker in the NARR. This band is reflecting convection due to fast-moving synoptic weather systems or propagating mesoscale convective systems (MCSs) around the northeastern periphery of the monsoon ridge. These MCSs typically originate as diurnal convection over the Rocky Mountains that propagate through the Great Plains and into

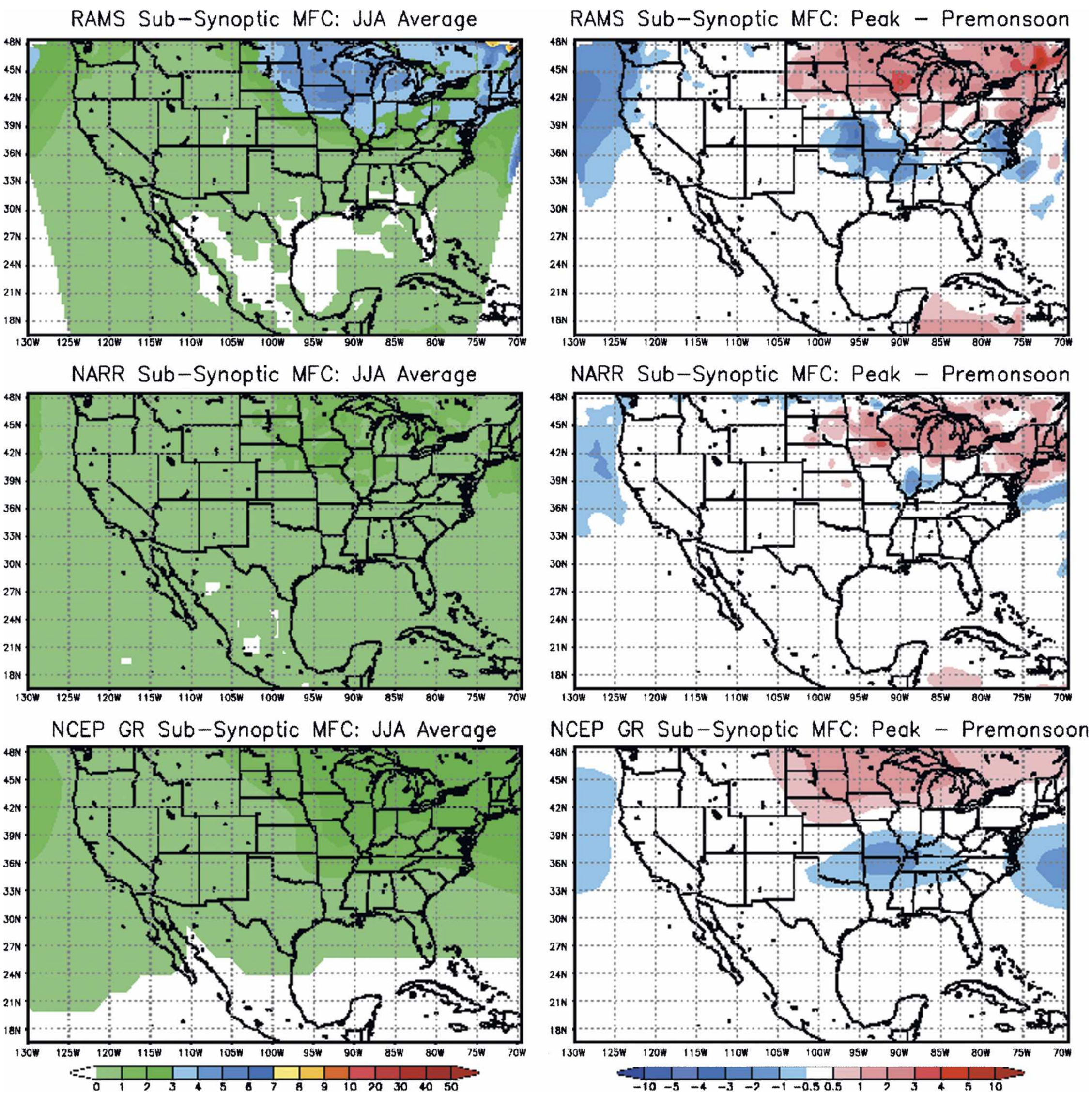

FIG. 12. As in Fig. 11 but for the subsynoptic (1.5–3 day) band.

the Midwest (Cotton et al. 1983; Tripoli and Cotton 1989; Wetzel et al. 1983; Carbone et al. 2002). As the monsoon ridge evolves through the summer, the peak minus premonsoon difference shows that this mode decreases in strength in the south-central United States and increases in strength in the upper Midwest. This mode is partially responsible for the rainfall maximum in the central United States in late spring to early summer.

The synoptic mode of MFC is shown in Fig. 13. Like the diurnal cycle, this mode has the largest weighted spectral power in the southeast United States, Mexico, and western United States and reflects the passage of westward propagating disturbances around the southern periphery of the monsoon ridge (i.e., inverted troughs, tropical easterly waves, and possibly tropical cyclones). The monsoon minus premonsoon difference in the synoptic MFC clearly shows that these westward propagating disturbances affect convection in central and southern Mexico in the premonsoon period and then the southeast United States and core monsoon region during the peak of the monsoon. In the core monsoon region, these disturbances enhance the diurnally forced convection and allow it to more readily propagate off the elevated terrain and organize into MCSs, such as demonstrated in radar observations (Carbone et al. 2002). Such bursts of convection are reflected in a significant spectral peak in rainfall in the 12–18-day band in Arizona (e.g., Cavazos et al. 2002). If they are propagating westward off the SMO, the MCSs may trigger moisture surges into the Gulf of California.

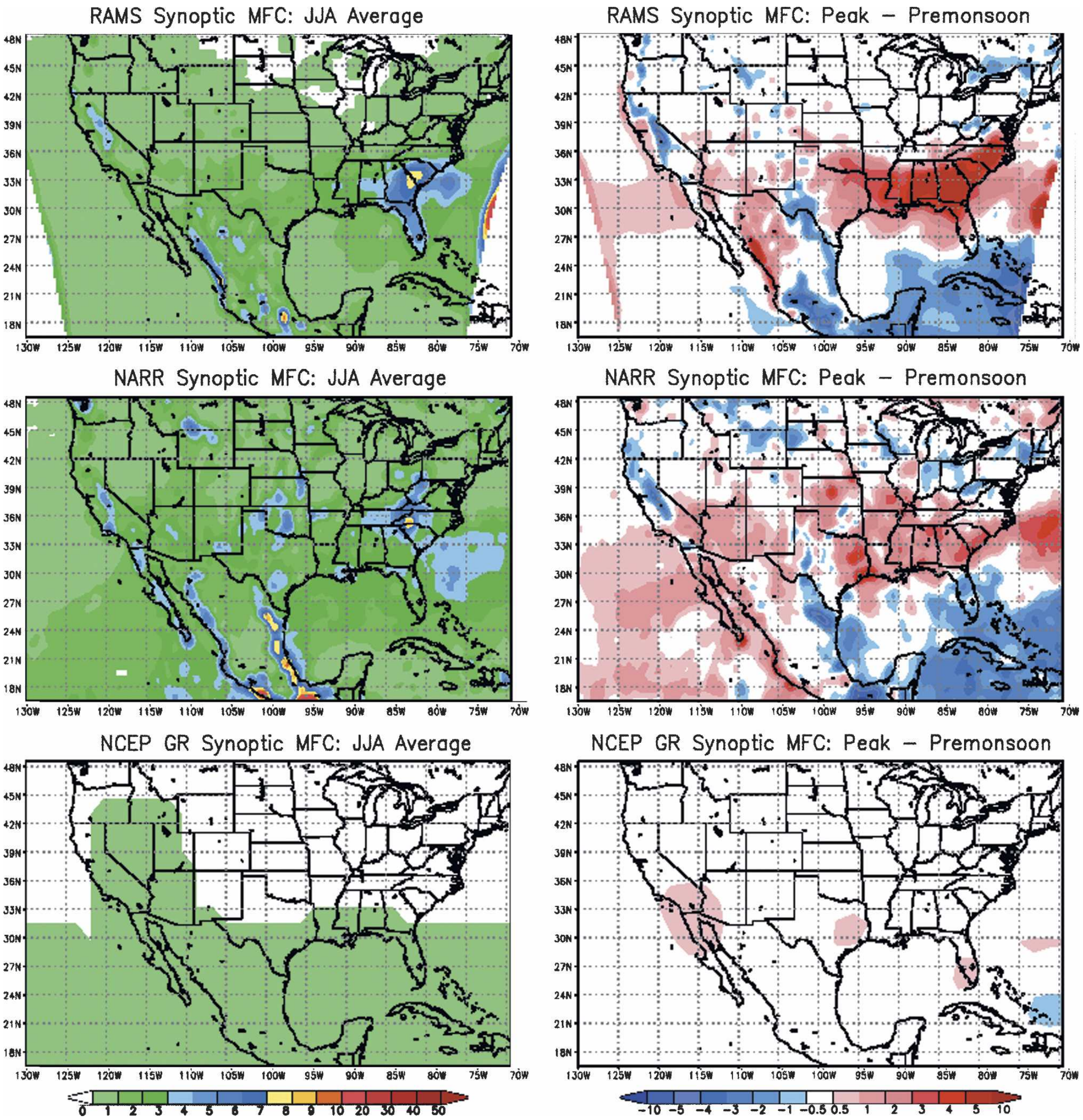

FIG. 13. As in Fig. 11 but for the synoptic (4–15 day) band.

A major surge may be triggered if these events are preceded by the passage of a westerly trough (Adams and Comrie 1997; Stensrud et al. 1997) or a tropical cyclone near the Gulf of California (R. Maddox 2006, personal communication). As with the diurnal cycle, the NCEP GR does a poor job of capturing variability of MFC in this band.

Figure 14 shows the fraction of weighted spectral power of each band relative to the sum of all the bands averaged over the summer for RAMS and NARR. Though the diurnal cycle is clearly the dominant mechanism of summer rainfall, lower frequency modes of convection do significantly impact the summer rainfall in areas at a distance from elevated terrain. The subsynoptic MFC fraction suggests that approximately 20%–60% of summer rainfall in the Midwest may be due to MCSs, which matches earlier estimates based on analysis of precipitation (Fritsch et al. 1986). The synoptic MFC fraction illustrates that MCS and gulf surge-related rainfall in the core monsoon region become more important at the northernmost extent of the core monsoon region, especially Arizona, and at lower elevation. Previous RCM studies have shown that gulf-surge-related precipitation accounts for the majority of rainfall in the western part of the state toward the Colorado River valley (Berbery and Fox-Rabinovitz 2003).

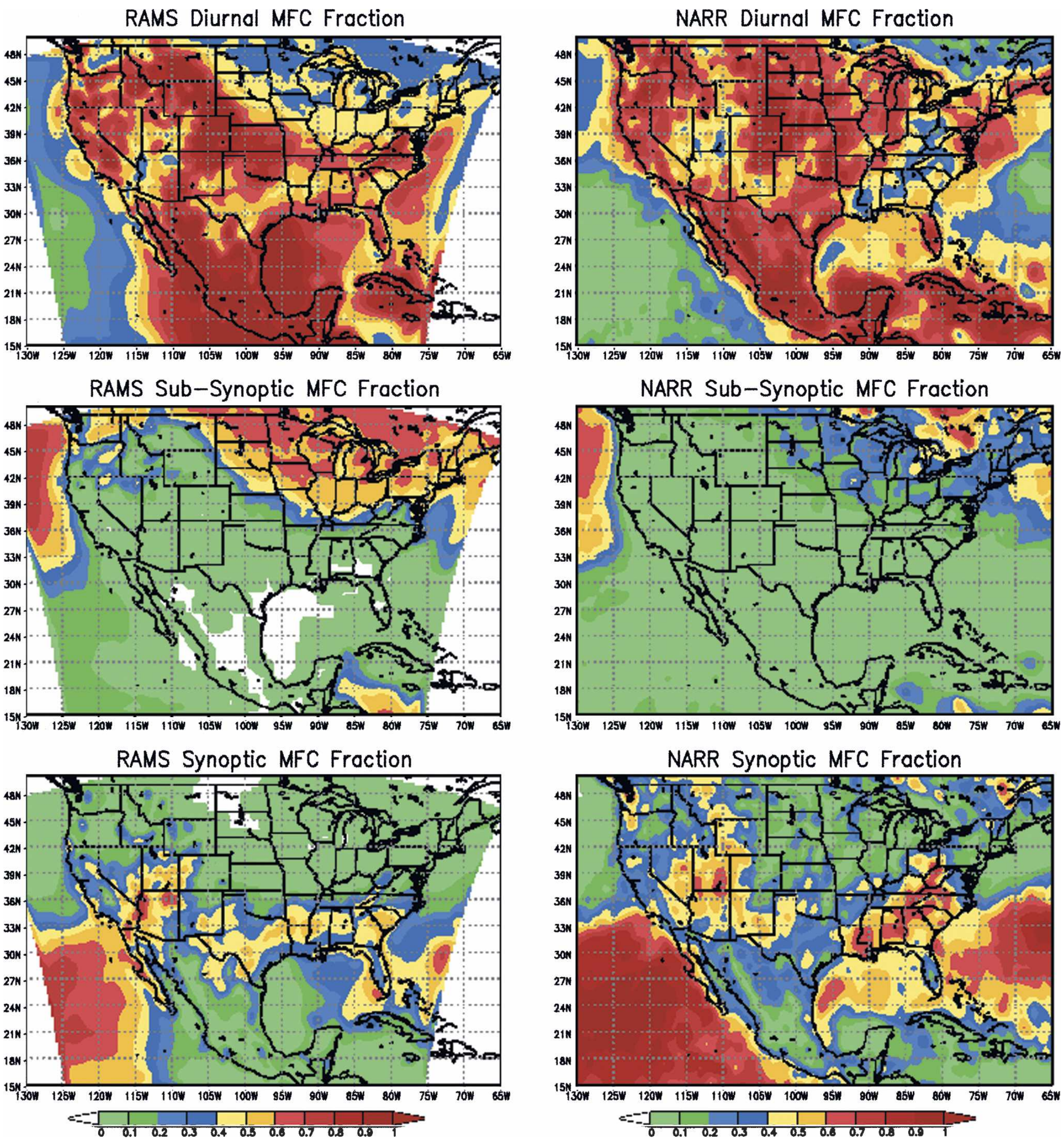

FIG. 14. Summer average fraction of MFC in the given spectral band relative to the total of the three bands for RAMS and NARR. Shading indicated by the color bars.

Given the difficulty in simulating gulf surges in RAMS in the present configuration, further research with finer-resolution RCMs is necessary to clarify its role.

7. Discussion

This evaluation of North American summer climatology with RAMS, combined with the NARR, allows us to define some essential features of North American summer climate that necessarily require a RCM to be properly represented. In agreement with previous studies, the most important value-added component by the RCM is the diurnal cycle of convective rainfall. The addition of high-resolution surface information is necessary to simulate the terrain-induced mesoscale circulations, especially in the core monsoon region and central United States. Because global atmospheric reanalyses (GR) and GCMs cannot properly represent the diurnal cycle, they cannot resolve the major and abrupt climatological transitions in North American summer rainfall. The diurnal cycle necessarily affects the lower frequency modes of convective rainfall because these strongly depend on terrain-induced convection.

The representation of the convective rainfall will affect how the surface energy budget and mean surface air temperatures are represented in the RCM. In areas where most of the monsoon rainfall is due to diurnal convection, the regular and steady daily rainfall that occurs after monsoon onset is sufficient to lower the Bowen ratio, so mean surface air temperature decreases. Where rainfall is more intraseasonally variable, the mean surface temperatures do not exhibit a decrease subsequent to monsoon onset. Thus, the climatological character of the NAMS in the United States is distinct from that in Mexico. Castro et al. (2007) will show that the same holds true with respect to climate variability.

In spite of the ability of both RAMS and NARR to successfully represent many aspects of North American summer climate, each model had its own unique deficiencies and neither should be considered a "perfect" product. The most important point to highlight is the misrepresentation of the Baja LLJ in both models. The failure to reproduce the salient features of the Baja LLJ in RAMS may be due to a combination of factors in the RAMS experimental design. Though other models have achieved a reasonable representation of the Baja LLJ at comparable grid spacing, a grid spacing of 35 km may not be sufficient for RAMS. The simplifications in the representation of precipitation may also be a factor. Specifically the model did not include an explicit microphysical representation of the precipitation. A test simulation with a 5-km nested grid over the Gulf of California with explicit microphysics performed much better.

RAMS represented aspects of summer precipitation well in some regions but not in others. The simulation of summer precipitation by RAMS in North America is on par with other RCMs referenced herein. As the sensitivity studies demonstrate, it is difficult to define the "correct" RCM configuration that will compare universally well with observations. RAMS improved the representation of precipitation, as compared to the NCEP–NCAR global reanalysis, in regions most significantly impacted by the NAMS. In addition, what is the "correct" observed precipitation to compare model results against? Should the CPC gauge observations be really trusted as "ground truth" in Mexico? Or are RCMs actually doing better than observations would currently suggest? Improving the estimation of precipitation in this region in observations and regional models was one of the major goals of the recent NAME and is an area of ongoing research.

8. Summary

In this Part I of the study, 53 years of the NCEP–NCAR Reanalysis I have been dynamically downscaled using RAMS to generate a RCM summer climatology of the contiguous United States and Mexico. Data from the RAMS simulations were compared to the recently released NARR, as well as observed precipitation and temperature data. The RAMS simulations show the value added by using a RCM in process mode to represent North American summer climate beyond the driving GR. Because of its enhanced representation of the surface boundary, the diurnal cycle of convective rainfall is present. This diurnal cycle largely governs transitions associated with evolution of the North American monsoon, in terms of rainfall, the surface energy budget, and surface temperature. The lower frequency modes of convective rainfall, though weaker, account for rainfall variability at a remote distance from elevated terrain. As in previous studies, RAMS RCM-generated precipitation is overestimated compared to observations. The Great Plains LLJ was also well represented in both RAMS and NARR, but the Baja LLJ and associated gulf surges were not.

Acknowledgments. This research was funded by NOAA Grant NA17RJ1228 Amendment 6 and NASA Grant NGT5-30344. The authors thank Dr. Lixin Lu for providing SOD data. The authors also thank the Distributed Archive Data Center at the Goddard Space Flight Center, Greenbelt, Maryland, for distributing the satellite-derived precipitation data. Dr. William R. Cotton, two anonymous reviewers, and *Journal of Climate* editor Dr. David Straus provided constructive comments that improved the manuscript.

REFERENCES

Adams, D. K., and A. C. Comrie, 1997: The North American monsoon. *Bull. Amer. Meteor. Soc.,* **78,** 2197–2213.

Adegoke, J. O., R. A. Pielke Sr., J. Eastman, R. Mahmood, and K. G. Hubbard, 2003: Impact of irrigation on midsummer surface fluxes and temperature under dry synoptic conditions: A regional atmospheric model study of the U.S. High Plains. *Mon. Wea. Rev.,* **131,** 556–564.

Anderson, B. T., 2002: Regional simulations of intraseasonal variations in the summertime hydrologic cycle over the southwestern United States. *J. Climate,* **15,** 2282–2299.

——, J. O. Roads, S. Chen, and H. H. Juang, 2000: Regional simulation of the low-level monsoon winds over the Gulf of California and the southwestern United States. *J. Geophys. Res.,* **105,** 24 455–24 467.

——, H. Kanamaru, and J. O. Roads, 2004: The summertime atmospheric hydrologic cycle over the southwestern United States. *J. Hydrometeor.,* **5,** 679–692.

Arkin, P. A., 1979: The relationship between the fractional coverage of high cloud and rainfall accumulations during GATE over the B-scale array. *Mon. Wea. Rev.,* **107,** 1382–1387.

Barlow, M., S. Nigam, and E. H. Berbery, 1998: Evolution of the North American monsoon system. *J. Climate,* **11,** 2238–2257.

Berbery, E. H., 2001: Mesoscale moisture analysis of the North American monsoon. *J. Climate,* **14,** 121–137.

——, and M. S. Fox-Rabinovitz, 2003: Multiscale diagnosis of the North American monsoon system using a variable resolution GCM. *J. Climate,* **16,** 1929–1947.

Brubaker, K. L., P. A. Dirmeyer, A. Sundradiat, B. S. Levey, and F. Bernal, 2001: A 36-yr climatological description of the evaporative sources of warm-season precipitation in the Mississippi River basin. *J. Hydrometeor.,* **2,** 537–557.

Bryson, R. A., and W. P. Lowry, 1955: The synoptic climatology of the Arizona summer precipitation singularity. *Bull. Amer. Meteor. Soc.,* **36,** 329–339.

Carbone, R. E., J. D. Tuttle, D. A. Ahijevych, and S. B. Trier, 2002: Inferences of predictability associated with warm season precipitation episodes. *J. Atmos. Sci.,* **59,** 2033–2056.

Castro, C. L., 2005: Investigation of the summer climate of North America: A regional atmospheric modeling study. Ph.D. dissertation, Colorado State University, 210 pp.

——, T. B. McKee, and R. A. Pielke Sr., 2001: The relationship of the North American monsoon to tropical and North Pacific sea surface temperatures as revealed by observational analyses. *J. Climate,* **14,** 4449–4473.

——, W. Y. Y. Cheng, A. B. Beltrán, R. A. Pielke Sr., and W. R. Cotton, 2002: The Incorporation of the Kain-Fritsch cumulus parameterization scheme in RAMS with a terrain-adjusted trigger function. *Proc. Fifth RAMS Users and Related Applications Workshop,* Santorini, Greece, ATMET, Inc.

——, R. A. Pielke Sr., and G. Leoncini, 2005: Dynamical downscaling: Assessment of value restored and added using the Regional Atmospheric Modeling System (RAMS). *J. Geophys. Res.,* **110,** D05108, doi:10.1029/2004JD004721.

——, ——, J. O. Adegoke, S. D. Schubert, and P. J. Pegion, 2007: Investigation of the summer climate of the contiguous United States and Mexico using the Regional Atmospheric Modeling System (RAMS). Part II: Model climate variability. *J. Climate,* **20,** 3866–3887.

Cavazos, T., A. C. Comrie, and D. M. Liverman, 2002: Intraseasonal variability associated with wet monsoons in southeast Arizona. *J. Climate,* **15,** 2477–2490.

Chen, C., and W. R. Cotton, 1983: A one-dimensional simulation of the stratocumulus-capped mixed layer. *Bound.-Layer Meteor.,* **25,** 298–321.

——, and ——, 1987: The physics of the marine stratocumulus-capped mixed layer. *J. Atmos. Sci.,* **44,** 2951–2977.

Cotton, W. R., R. L. George, P. J. Wetzel, and R. L. McAnelly, 1983: A long-lived mesoscale convective complex. Part I: The mountain-generated component. *Mon. Wea. Rev.,* **111,** 1893–1918.

——, and Coauthors, 2003: RAMS 2001: Current status and future directions. *Meteor. Atmos. Phys.,* **82,** 5–29.

Davies, H. C., 1976: A lateral boundary formulation for multi-level prediction models. *Quart. J. Roy. Meteor. Soc.,* **102,** 405–418.

Diffenbaugh, N. S., J. S. Pal, R. J. Trapp, and F. Giorgi, 2005: Fine-scale processes regulate the response of extreme events to global climate change. *Proc. Natl. Acad. Sci. USA,* **102,** 15 774–15 778.

Douglas, M. W., 1995: The summertime low-level jet over the Gulf of California. *Mon. Wea. Rev.,* **123,** 2334–2347.

——, R. A. Maddox, and K. Howard, 1993: The Mexican monsoon. *J. Climate,* **6,** 1665–1677.

Eastman, J. L., M. B. Coughenour, and R. A. Pielke Sr., 2001: Does grazing affect regional climate? *J. Hydrometeor.,* **2,** 243–253.

Fritsch, J. M., R. J. Kane, and C. R. Chelius, 1986: The contribution of mesoscale convective weather systems to the warm-season precipitation in the United States. *J. Climate Appl. Meteor.,* **25,** 1333–1345.

Gilman, D., P. Fuglister, and J. M. Mitchell, 1963: On the power spectrum of red noise. *J. Atmos. Sci.,* **20,** 182–184.

Gochis, D. J., W. J. Shuttleworth, and Z. L. Yang, 2002: Sensitivity of the modeled North American monsoon regional climate to convective parameterization. *Mon. Wea. Rev.,* **130,** 1282–1298.

——, ——, and ——, 2003: Hydrometeorological response of the modeled North American monsoon to vonvective parameterization. *J. Hydrometeor.,* **4,** 235–250.

Gutzler, D., and Coauthors, 2004: *The North American Monsoon Model Assessment Project (NAMAP).* NCEP Climate Prediction Center Atlas 11, 32 pp.

Higgins, R. W., J. E. Janowiak, and Y. Yao, 1996: *A Gridded Hourly Precipitation Data Base for the United States (1963–1993).* NCEP Climate Prediction Center Atlas 1, 47 pp.

——, Y. Yao, and X. L. Wang, 1997a: Influence of the North American monsoon system on the U.S. summer precipitation regime. *J. Climate,* **10,** 2600–2622.

——, ——, E. S. Yarosh, J. E. Janowiak, and K. C. Mo, 1997b: Influence of the Great Plains low-level jet on summertime precipitation and moisture transport over the central United States. *J. Climate,* **10,** 481–507.

——, Y. Chen, and A. V. Douglas, 1999: Interannual variability of the North American warm season precipitation regime. *J. Climate,* **12,** 653–680.

Huang, J., H. M. Van den Dool, and K. P. Georgarakos, 1996: Analysis of model-calculated soil moisture over the United States (1931–1993) and application to long-range temperature forecasts. *J. Climate,* **9,** 1350–1362.

Kain, J. S., 2004: The Kain–Fritsch convective parameterization scheme: An update. *J. Appl. Meteor.,* **43,** 170–181.

——, and J. M. Fritsch, 1993: Convective parameterization for mesoscale models: The Kain-Fritsch scheme. *The Representation of Cumulus Convection in Numerical Models, Meteor. Monogr.,* No. 24, Amer. Meteor. Soc., 165–170.

Kalnay, E., and Coauthors, 1996: The NCEP/NCAR 40-Year Reanalysis Project. *Bull. Amer. Meteor. Soc.,* **77,** 437–471.

Kanamitsu, M., and K. C. Mo, 2003: Dynamical effect of land surface processes on summer precipitation over the southwestern United States. *J. Climate,* **16,** 496–503.

——, W. Ebisuzaki, J. Woollen, S.-K. Yang, J. J. Hnilo, M. Fiorino, and G. L. Potter, 2002: NCEP–DOE AMIP-II Reanalysis (R-2). *Bull. Amer. Meteor. Soc.,* **83,** 437–471.

Li, J., X. Gao, R. A. Maddox, and S. Sarooshian, 2004: Model study of evolution and diurnal variations of rainfall in the North American monsoon during June and July 2002. *Mon. Wea. Rev.,* **132,** 2895–2915.

Liang, X.-Z., L. Li, K. E. Kunkel, M. Ting, and J. X. L. Wang, 2004: Regional climate model simulation of U.S. precipitation during 1982–2002. Part I: Annual cycle. *J. Climate,* **17,** 3510–3529.

Liston, G. E., and R. A. Pielke Sr., 2001: A climate version of the Regional Atmospheric Modeling System. *Theor. Appl. Climatol.,* **68,** 155–173.

Maurer, E. P., A. W. Wood, J. C. Adam, D. P. Lettenmaier, and B. Nijssen, 2002: A long-term hydrologically based dataset of land surface fluxes and states for the conterminous United States. *J. Climate,* **15,** 3237–3251.

Mellor, G. L., and T. Yamada, 1974: A hierarchy of turbulence closure models for planetary boundary layers. *J. Atmos. Sci.,* **31,** 1791–1806.

Mesinger, F., and Coauthors, 2006: North American regional reanalysis. *Bull. Amer. Meteor. Soc.,* **87,** 343–360.

Miguez-Macho, G., G. L. Stenchikov, and A. Robock, 2005: Regional climate simulations over North America: Interactions of local processes with improved large-scale flow. *J. Climate,* **18,** 1227–1246.

Mo, K. C., M. Chelliah, M. Carrera, R. W. Higgins, and W. Ebisuzaki, 2005: Atmospheric moisture transport over the United States and Mexico as evaluated from the NCEP regional reanalysis. *J. Hydrometeor.,* **6,** 710–728.

Pielke, R. A., Sr., 2002: *Mesoscale Meteorological Modeling.* 2d ed. Academic Press, 676 pp.

——, and Coauthors, 1992: A comprehensive meteorological modeling system—RAMS. *Meteor. Atmos. Phys.,* **49,** 69–91.

Reynolds, R. W., and T. M. Smith, 1994: Improved global sea surface temperature analyses using optimum interpolation. *J. Climate,* **7,** 929–948.

Rogers, P. J., 2005: An observational analysis of two gulf surge events during the North American Monsoon Experiment. M.S. thesis, Dept. of Atmospheric Science, Colorado State University, 153 pp.

Saleeby, S. M., and W. R. Cotton, 2004: Simulations of the North American monsoon system. Part I: Model analysis of the 1993 monsoon season. *J. Climate,* **17,** 1997–2018.

Schmitz, J. T., and S. Mullen, 1996: Water vapor transport associated with the summertime North American monsoon as depicted by ECMWF analyses. *J. Climate,* **9,** 1621–1634.

Smagorinsky, J., 1963: General circulation experiments with the primitive equations: Part I. The basic experiment. *Mon. Wea. Rev.,* **91,** 99–164.

Stensrud, D. J., R. Gall, and M. Nordquist, 1997: Surges over the Gulf of California during the Mexican monsoon. *Mon. Wea. Rev.,* **125,** 417–437.

Tripoli, G. J., and W. R. Cotton, 1980: A numerical investigation of the several factors contributing to the observed variable intensity of deep convection over south Florida. *J. Appl. Meteor.,* **19,** 1037–1063.

——, and ——, 1989: Numerical study of an observed orogenic mesoscale convective system. Part 1: Simulated genesis and comparison with observations. *Mon. Wea. Rev.,* **117,** 273–304.

Uppala, S. M., and Coauthors, 2005: The ERA-40 re-analysis. *Quart. J. Roy. Meteor. Soc.,* **131,** 2961–3012.

von Storch, H., and F. W. Zwiers, 1999: *Statistical Analysis in Climate Research.* Cambridge University Press, 484 pp.

Walko, R. L., and Coauthors, 2000: Coupled atmosphere–biology–hydrology models for environmental modeling. *J. Appl. Meteor.,* **39,** 931–944.

Wetzel, P. J., W. R. Cotton, and R. L. McAnelly, 1983: A long-lived mesoscale convective complex. Part II: Evolution and structure of the mature complex. *Mon. Wea. Rev.,* **111,** 1919–1937.

Xu, J., and E. Small, 2002: Simulatimg summertime rainfall variability in the North American monsoon region: The influence of convection and radiation parameterizations. *J. Geophys. Res.,* **107,** 4727, doi:10.1029/2001JD002047.

——, X. Gao, J. Shuttleworth, S. Sarooshian, and E. Small, 2004: Model climatology of the North American monsoon onset period during 1980–2001. *J. Climate,* **17,** 3892–3906.

Yang, Z.-L., D. Gochis, W. J Shuttleworth, and G.-Y. Niu, 2003: The impact of sea surface temperature on the North American monsoon: A GCM study. *Geophys. Res. Lett.,* **30,** 1033, doi:10.1029/2002GL015628.